

Stable 1:2 Resonant Periodic Orbits in Elliptic Three-Body Systems

Nader Haghighipour^{1,2}, Jocelyn Couetdic^{3,4}, Ferenc Varadi⁴ and William B. Moore^{4,5}

ABSTRACT

The results of an extensive numerical study of the periodic orbits of planar, elliptic restricted three-body planetary systems consisting of a star, an inner massive planet and an outer mass-less body in the external 1:2 mean-motion resonance are presented. Using the method of differential continuation, the locations of the resonant periodic orbits of such systems are identified and through an extensive study of their phase-parameter space, it is found that the majority of the resonant periodic orbits are unstable. For certain values of the mass and the orbital eccentricity of the inner planet, however, stable periodic orbits can be found. The applicability of such studies to the 1:2 resonance of the extrasolar planetary system GJ876 is also discussed.

Subject headings: celestial mechanics, minor planets, asteroids, planetary systems, solar system: general

1. Introduction

It is well known that orbital or mean-motion resonances are of great importance in the dynamics of planetary and satellite systems. Resonances drive the dynamical evolution of

¹Dearborn Observatory, Northwestern University, Evanston, IL 60208.

²Department of Terrestrial Magnetism and the NASA Astrobiology Institute, Carnegie Institution of Washington, 5241 Broad Branch Road, Washington, DC 20015; nader@dtm.ciw.edu.

³Option Physique Appliquée, Ecole Centrale Paris, Grande voie des vignes, 92295 Chatenay-Malabry Cedex, France; couetdj3@cti.ecp.fr.

⁴Institute of Geophysics and Planetary Physics and the NASA Astrobiology Institute, UCLA, 405 Hilgard Avenue, Los Angeles, CA 90095-1567; varadi@ucla.edu.

⁵Department of Earth and Space Sciences, UCLA, 595 Charles Young Dr., Los Angeles, CA 90095-1567; bmoore@avalon.ess.ucla.edu.

such systems by creating regions of stability and instability in orbital phase space. Mean-motion resonances are usually associated with orbits whose geometrical configurations are periodically repeated. Such orbits, known as resonant periodic orbits (hereafter RPOs), are of particular interest since they define the structure of the associated resonance. The stability of an RPO implies that it may be a potential location for harboring an actual body. Unstable RPOs, on the other hand, provide pathways for dramatic orbital evolution of bodies and can also be used to explain chaotic motions (Varadi & Kaula 1999).

Until a few years ago, mean-motion resonances were found only in our solar system. Recent success of the precise radial velocity searches in detecting more than 100 extrasolar planets has extended the applicability of resonances to a broader context, several parsecs beyond the boundaries of our solar system.⁶ Among these planetary systems, GJ876 is a three-body system with two planets in a 1:2 resonance (Marcy et al. 2001) and 47 UMa has two planets that are a near 2:5 commensurability (Rivera & Haghighipour 2003). Because of the universal importance and applicability of resonances, it is of great value to study RPOs and investigate their dynamical stability.

The most widely known RPOs are the ones associated with the 1:1 resonance. In a three-body system, these RPOs are the Lagrangian points in a frame co-rotating with the major planet. In case of the three-body system of Sun, Jupiter and a test particle, the stable RPOs are located at $\pm 60^\circ$ with respect to the location of Jupiter on its orbit around the Sun. The roughly 1500 known Jupiter Trojan asteroids are the actual bodies that are trapped in the 1:1 resonance with Jupiter at these two locations.

Our knowledge of the RPOs of other orbital resonances is limited to only a few values of the eccentricity of the inner planet and its mass relative to the star. It is therefore essential to carry out studies similar to those for the 1:1 resonance for other mean-motion resonances and to explore their phase-parameter spaces for regions of stability. Such a study has been previously carried out by Varadi (1999) for the case of the 2:3 exterior resonance. In that paper, the method of differential continuation was employed to identify the regions of the phase-parameter space of planar, elliptic restricted three-body systems that correspond to stable orbits of the outer body while in the 2:3 resonance.

In this paper, we present the results of an extensive study of the RPOs of the exterior 1:2 resonance. The system of interest is planar, elliptic and restricted, with an inner massive planet (hereafter, the major planet) and an outer zero-mass particle. We employ the methodology of Varadi (1999) and vary the parameters of the system in a systematic way in order

⁶See exoplanets.org for a complete and up-to-date list of extarsolar planets with their corresponding references.

to identify its stable RPOs and their corresponding regions of stability in phase-parameter space.

A review of our methodology is presented in § 2. Section 3 presents the results of our numerical study and in § 4 we conclude by reviewing the results and discussing their implications to extrasolar planetary systems.

2. Methodology

Our method of identifying an RPO consists of two steps; search and continuation. To describe this process, we start by briefly reviewing the condition for an orbit to be periodic. Let us consider a planar, restricted three-body system with a mass-less particle in an exterior resonance with a major planet. If \mathbf{x} denotes the four-dimensional vector of the initial position and velocity of the outer particle, then after a certain number of orbits of the major planet, the particle’s position and velocity will be given by another vector $\mathbf{F}(\mathbf{x})$. The orbit is periodic if

$$\mathbf{F}(\mathbf{x}(\varepsilon), \varepsilon) - \mathbf{x}(\varepsilon) = 0, \quad (1)$$

where ε is a parameter of the system. For the systems considered here, ε can be taken to be the ratio of the mass of the major planet to that of the central star. The mapping \mathbf{F} is given by numerically integrating the equations of motions. Solution vectors \mathbf{x} of equation (1) represent RPOs of the system.

Equation (1) can be differentiated with respect to ε to obtain

$$\frac{d\mathbf{x}}{d\varepsilon} = -\left(\frac{d\mathbf{F}}{d\mathbf{x}} - \mathbf{I}\right)^{-1} \frac{d\mathbf{F}}{d\varepsilon}, \quad (2)$$

where \mathbf{I} is the identity matrix. Equation (2) involves the variational equations of the dynamics of the system. It leads to a complicated system of differential equations in which the independent variable is ε (Varadi 1999).

Equation (1) can, in principle, be solved by Newton’s method. Because the latter converges only for some vectors \mathbf{x} , due to the nonlinear nature of equation (1), many initial vectors have to be tried. For a chosen value of ε , we select random initial conditions, integrate the dynamical equations and if \mathbf{F} happens to be small, we apply Newton’s method to search for a nearby solution of equation (1). We then apply differential continuation (Keller 1977), i.e., solve equation (2), to follow the changes in the RPO due to varying ε .

We start our search for 1:2 resonant periodic orbits by choosing the semimajor axis of the outer body near its resonant value with the inner planet. The semimajor axis of the

inner planet is assumed to be equal to unity. Many possible configurations are considered in which the other orbital parameters of the outer body are chosen randomly. The inner planet is placed at either the peri- or the apocenter without any loss of generality. We integrate the system for two orbits of the inner planet and form the differences between the initial and the final position and velocity vectors of the outer body. When these differences are small, we apply Newton’s method to further reduce them. This process is repeated until these differences become so small that the orbit can be considered to be an RPO.

The ratio of the mass of the inner planet to the mass of the central star (μ) and also the orbital eccentricity of the inner planet (e) are the parameters of our system. During the process of differential continuation, we vary μ and e and solve equation (2) to obtain new RPOs along a path in (μ, e) space. To identify the regions of the phase-parameter space of the system which correspond to stable RPOs, we change μ and e systematically and criss-cross the (μ, e) space with paths of continuation along which the stability of RPOs is computed.

The stability of RPOs is examined by computing the eigenvalues of the monodromy matrix $d\mathbf{F}/d\mathbf{x}$ (Danby 1964; Golub & Van Loan 1996). Stable RPOs are centers of libration for nearby orbits. Unstable RPOs are associated with separatrix-like features (Guckenheimer & Holmes 1983). The eigenvalues of the monodromy matrix provide the frequency of libration associated with stable RPOs and also the Lyapunov exponent of the outer body when the RPO is unstable. The system is linearly (spectrally) stable if these eigenvalues are on the unit circle in the complex plane. There is usually a separation of time scales between fast and slow dynamics and both can correspond to either stable or unstable motions. The fast dynamics usually consists of motions which are also present in the case of a circular orbit for the major planet. When this fast motion is stable, we call it libration. The slow dynamics is associated with the effects of orbital eccentricity of the major planet. We call stable motions in this case secular librations and unstable ones secular instabilities. An RPO is unstable when either of the two motions is unstable.

3. Numerical Results

We studied the orbit of the outer body of our three-body system for different values of the mass-ratio μ and also different values of the orbital eccentricity of the inner planet, e . To describe the shape and the orientation of these orbits, we use

$$h = e \cos \varpi, \quad k = e \sin \varpi \tag{3}$$

$$h' = e' \cos \varpi', \quad k' = e' \sin \varpi', \tag{4}$$

where e' is the orbital eccentricity of the outer body and ϖ and ϖ' represent the longitudes of the pericenters of the inner planet and the outer body, respectively. In order to completely specify an RPO, one needs the h' , k' , semi-major axis and mean longitude of the RPO at a given orbital phase of the inner planet.

We performed an extensive initial numerical search for 1:2 resonant periodic orbits for several mass-ratios and orbital eccentricities of the inner planet. Once an RPO was found, we used its orbital parameters for starting the continuation process. Figure 1 shows the overall results of the continuation process for starting values of 0.001 and 0.1 for μ and e , respectively. For all the shown branches of continuation, we have we have $\varpi = 0$ and therefore $k = 0$ and $h = e$. For the same orbit of the inner planet, there can be several RPOs with different orbital elements on different branches. These branches are labeled according to the initial values of their h' and k' quantities. This method of labeling enables one to readily calculate the orbital eccentricity and the longitude of the pericenter of the outer body at the start of the continuation process. For instance, the branch labeled as $h'52k'16$ represents the result of continuation started from a resonant periodic orbit with $h' = 0.52$ and $k' = 0.16$. Such an orbit has an eccentricity equal to 0.544 and a longitude of pericenter equal to 17.1° .

One can see from Figure 1 that certain branches shown here appear to be connected, either through so-called turning points or via circular connection. To explain these cases, we recall that any continuation branch corresponds to a periodic orbit that has been continued from an initial RPO, for different values of the mass and the orbital eccentricity of the inner body. The continuation process can break down at points where the matrix $(d\mathbf{F}/d\mathbf{x} - \mathbf{I})$ becomes singular. When two branches of continuation meet at a point on the h' - h plane where $h \neq 0$, they are said to be connected through a turning point. Turning point is a general term indicating that a branch changes its direction, or in other word, at a turning point, the tangent line to the continuation branch will be vertical (e.g., Keller 1977). The two branches $h'15k'00$ and $h'59k'00$ are connected via a turning point. Figure 2 shows the changes of the different orbital parameters of the outer body for these two branches.

On the line $h = 0$, the matrix above is always singular due to the fact that the differential equations for the outer planet become time-independent. In this case, the variational equations transport the equations of motions invariantly along the orbit (e.g., Siegel & Moser 1971; Varadi 1999). A circular connection occurs when two branches of continuation meet on the $h = 0$ line. Branches $h'004k'00$ and $h'15k'00$, $h'59k'00$ and $h'-67k'00$, and also $h'-05k'-57$ and $h'52k'16$ are connected in this way. We also have to note that the matrix above can also become singular at bifurcation points, which is discussed in the context of stability analysis.

The continuation process, however, can sometimes pass through singularities without major difficulties. This is due to the fact that the particular singularities are handled gracefully by the numerical integrator used to solve equation (2). An example is the smooth connection between $h'004k'00$ and $h'15k'00$ in Figure 1. Eventually there is a singularity of some type through which continuation is not possible.

As mentioned above, periodic orbits of the outer body are labeled by their orbital elements at the pericenter passage of the inner planet. In the cases in which the continuation process can be extended beyond $h = 0$, i.e., beyond the orbit of the inner planet being circular, the pericenter and the apocenter of the inner planet exchange places. That is, pericenter becomes apocenter and vice versa. To assure that the orbital parameters of the outer body will still be calculated at the time of the pericenter passage of the inner planet, we integrate the equations of motion of the outer body for half of the orbital period of the inner planet and then rotate the coordinate systems in such a way that the pericenter of the inner planet is located in the positive direction of the x -axis. At the same time, since we are dealing with the 1:2 external resonance, the outer body travels only one-fourth of its orbit and one obtains a new set of orbital elements. Once the re-alignment process is completed, there will be two sets of orbital parameters associated with the outer body. We assure that these two sets describe orbits unambiguously by limiting the values of the mean longitude of the outer body, λ' . In this study $-90^\circ < \lambda' < 90^\circ$. The re-alignment correction becomes necessary when the orbital parameters of the outer body undergo sudden changes during the passage of the inner planet through a circular orbit. Figure 3 shows such changes for the re-aligned and non-realigned values of h and h' for two circularly connected branches of $h'004k'00$ and $h'15k'00$.

As mentioned earlier, Figure 1 provides an overall view of the different continuation branches for a specific value of the inner planet's mass. When the latter is also varied, the branches become leaves parameterized by the mass and the eccentricity of the inner planet. In order to explore these leaves, the (μ, e) space is criss-crossed with continuation paths. Along these paths, μ and e are assumed to depend on a common independent variable. The derivatives of μ and e with respect to the independent variable are prescribed to yield the desired continuation path. Since the actual variable used in the continuation is not e but the velocity of the inner planet at peri- or apocenter, the paths will have slight curvature (see also Varadi 1999).

We also studied the phase-parameter space of the system, in search of regions corresponding to stable resonant periodic orbits, for all different branches of Figure 1. In most cases, the RPOs were unstable. Figure 4 shows a criss-crossing of the (μ, e) space with continuation paths of the RPO designated as $h'004k'00$. An interesting feature of this case

is that the RPO can be stable in the horizontal directions while unstable in the vertical one. We note that planar motions, such as the RPOs in this study, can be unstable to vertical perturbations. Straightforward algebra reveals that the variational equations decouple the linearized dynamics of horizontal and vertical motions. Hence it is relatively simple to analyze vertical stability.

In Figure 5 and others of the same type, the quantities on the vertical axes represent either frequencies of libration or Lyapunov exponents, both computed from the eigenvalues of the monodromy matrix. When the plotted value is positive, it is known as the libration frequency. When the plotted values is negative, its absolute value is conventionally called Lyapunov exponent. Since both quantities have units of time, it is possible to plot them on the same axis. Varadi (1999) provides some clarifying examples. The orbit is linearly stable if all plotted values are positive and it is unstable otherwise. Since the linearized equations are uncoupled for horizontal and vertical motions, there is a single frequency of libration or Lyapunov exponent associated with the vertical motions. The horizontal motions are associated with a pair of quantities, each being either frequency of libration or Lyapunov exponent.

In Figure 5, we have plotted frequencies of librations or Lyapunov exponents along the vertical continuation path $e = 0.5$ in Figure 4. For the values of the mass-ratio, μ , considered in Figure 4, the orbit is unstable. From Figure 5a, one can see that while this instability is sustained along the vertical direction and for all values of μ , the orbit becomes horizontally stable when $0.0091 \leq \mu \leq 0.03$ and $0.099 \leq \mu \leq 0.115$.

Figure 6 shows similar criss-crossing analysis for the continuation branch of the RPO $h'-05k'-57$. The system, in this case, reveals a region of stability with a distinct boundary from its large region of instability. The frequencies of librations or Lyapunov exponents of the system for different values of the mass-ratio μ and the orbital eccentricity of the inner planet are shown in Figures 7, 8 and 9. As shown in Figure 7, the orbit of the outer planet is stable along the horizontal line of $\mu = 0.001$ in Figure 6, for all values of the orbital eccentricity of the outer planet less than 0.57. Along a vertical line such as $e = 0.5$ in Figure 6, the system is stable for all values of the mass-ratio less than 0.0014 (Figure 8). Figure 9 shows frequencies of librations or Lyapunov exponents of the orbit of the outer body for the continuation branch in which the orbital eccentricity and the mass-ratio of the inner planet increase in steps of 0.01 and 0.001, respectively. The continuation path corresponding to this figure has been denoted by **X** in Figure 6. As shown in Figure 9, the orbit of the outer planet is stable for the values of the mass-ratio μ less than 0.005 and it becomes unstable for its larger values.

Figure 6 also shows that at higher values of the eccentricity of the inner planet, the

stability of the system requires lower mass ratios implying that the RPOs of a system with a more massive inner planet in a 1:2 exterior resonance are most stable when the orbit of the inner planet is closer to a circular orbit. The actual boundaries of stable regions can be different for different resonances and different leaves of the same resonance. For instance, the case of the 2:3 external resonance has a small wedge of instability (Varadi 1999).

Figures 10a and b show the different RPOs of such a system for the mass-ratio of 0.001 and different values of the inner planet’s orbital eccentricity. It is worth noting that for these stable orbits, the pericenter directions of the inner and outer planets are not aligned. The existence of a similar asymmetry of stable RPOs has also been suggested in the context of the Galilean satellites (Greenberg 1987).

4. Discussion

We presented the results of a systematic search for stable resonant periodic orbits of planar, elliptic and restricted three-body systems in the exterior 1:2 resonance. Our approach in this paper toward the understanding of orbital resonances provides fundamental information on their structures. Stable periodic orbits are centers of librations whose periods are also obtained, at least for small amplitudes, from our stability computations.

Using the method of differential continuation, we examined the phase-parameter space of the system for different values of the mass-ratio and the orbital eccentricity of the inner planet. In the majority of the cases, the RPOs were unstable. We were, however, able to show that stable resonant periodic orbits can be found when the mass and the orbital eccentricity of the inner planet are within a certain range (Figure 6).

Our initial search for RPOs also covered the internal 2:1 resonance. We have not found any RPOs, either stable or unstable, in this case. This can have significant implications for the 2:1 Kirkwood gap in the asteroid belt. It might be possible to arrive at an explanation of the gap in terms of the fundamental properties of the Sun-asteroid-Jupiter three-body system. This approach would be an alternative to the one adopted by Moon, Morbidelli & Milgiorini (1998) which employ elaborate physical models.

The apparent lack of RPOs in the internal 2:1 resonance also raises questions regarding the same resonance in the full three-body system, i.e., when the mass of the outer body is non-zero. As the latter increases and the mass of the inner body decreases, the system passes from external resonance to internal. Along the way, one should find the limits of masses for which stable RPOs exist. Such studies will have immediate applications to some of the recently discovered extrasolar planetary systems such as GJ876 in which two planets

are locked in a near 1:2 resonance.

We benefited from stimulating conversations with S. Peale. This work was partially supported by NASA Astrobiology Institute under grants NCC2-1056 (N.H.) and NCC2-1050 (J.C. and F.V.) and also by NASA NAG grant 5-11691 (F.V. and W.B.M.).

REFERENCES

- Danby, J. M. A. 1964, *AJ*, 69, 165
- Golub, G. H., & Van Loan, C. F. 1996, *Matrix Computations* (Baltimore, Johns Hopkins Univ. Press)
- Greenberg, R. 1987, *Icarus*, 70, 334
- Guckenheimer, J., & Holmes, P. 1983, *Nonlinear Oscillations, Dynamical Systems, and Bifurcations of Vector Fields*, (New York, Springer)
- Keller, H. B. 1977, in *Applications of Bifurcation Theory*, ed. P. H. Rabinowitz (London, Academic Press)
- Marcy, G. W., Butler, R. P., Fischer, D. A., Vogt, S. S., Lissauer, J. J., & Rivera, E. J. 2001, *ApJ*, 556, 296
- Moon, M., Morbidelli, A., & Milgiorini, F. 1998, *Icarus*, 135, 458
- Rivera, E. J., & Haghighipour, N. in *ASP Conf. Ser. Scientific Frontiers in Research on Extrasolar Planets*, ed D. Deming & S. Seager (San Francisco, ASP), in press
- Siegel, C. L., & Moser, J. K. 1971, *Lectures in Celestial Mechanics* (New York: Springer)
- Varadi, F., & Kaula, W. M. 1999, *Planet. Space Sci.*, 47, 997
- Varadi, F. 1999, *AJ*, 118, 2526

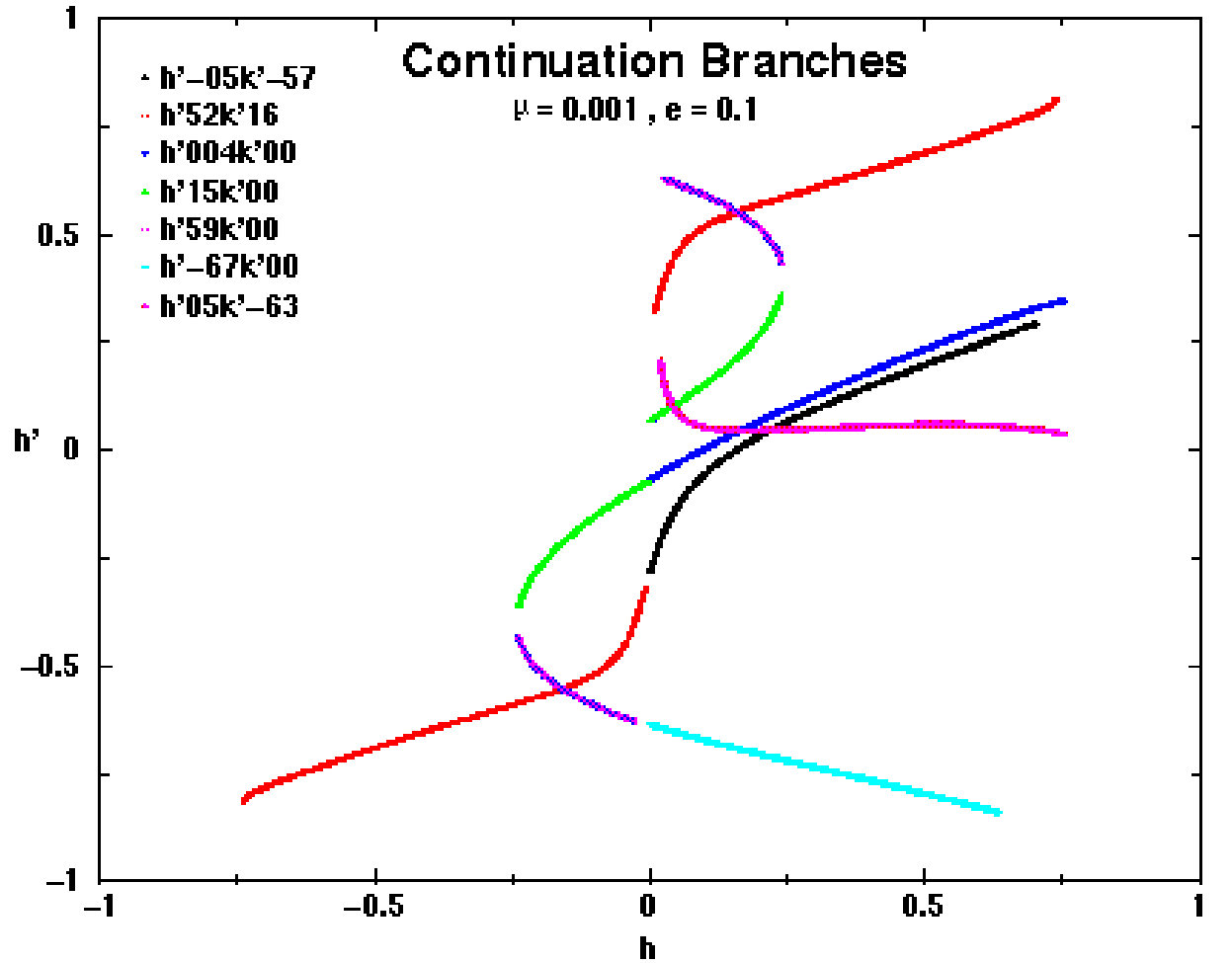


Fig. 1.— Structure of the continuation branches for different values of the orbital eccentricity of the outer body. Each branch represents the results of the continuation process started from an RPO with the given values of h' and k' . The mass-ratio and the orbital eccentricity of the inner planet at the start of the continuation process were $\mu=0.001$ and $e=0.1$, respectively.

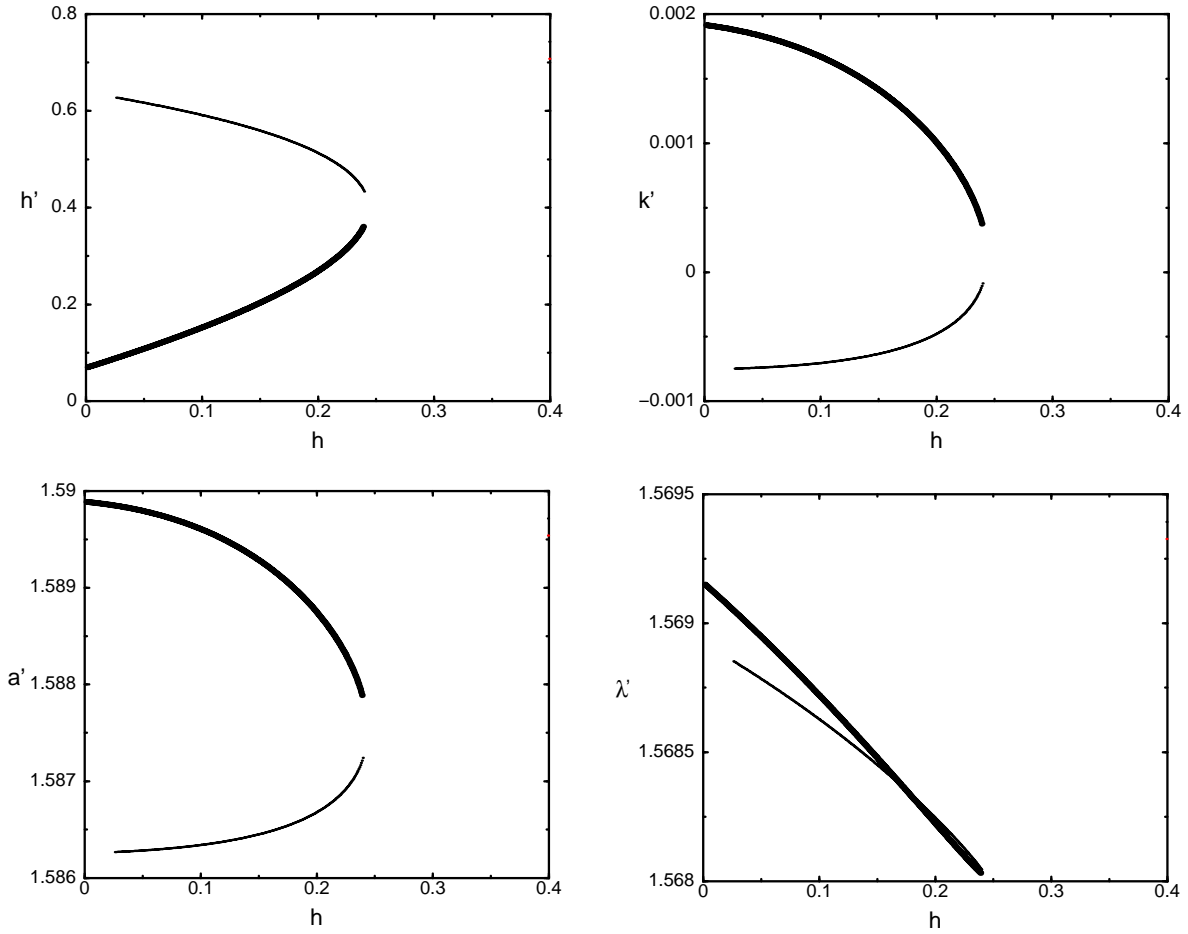


Fig. 2.— Graphs of the orbital parameters of the outer body versus h for turning-points connected continuation branches $h'15k'00$ (thick line) and $h'59k'00$ (thin line). The quantity λ' is the mean longitude of the outer body. The starting values of μ and e for all these graphs are equal to 0.001 and 0.1, respectively.

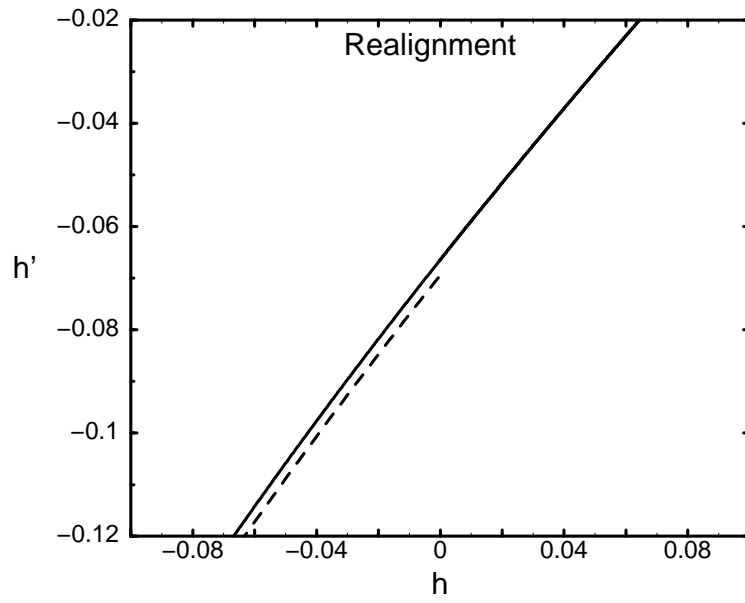


Fig. 3.— Graph of h' versus h for two circularly connected branches $h'004k'00$ and $h'15k'00$ before re-alignment (solid line) and after re-alignment (dashed line).

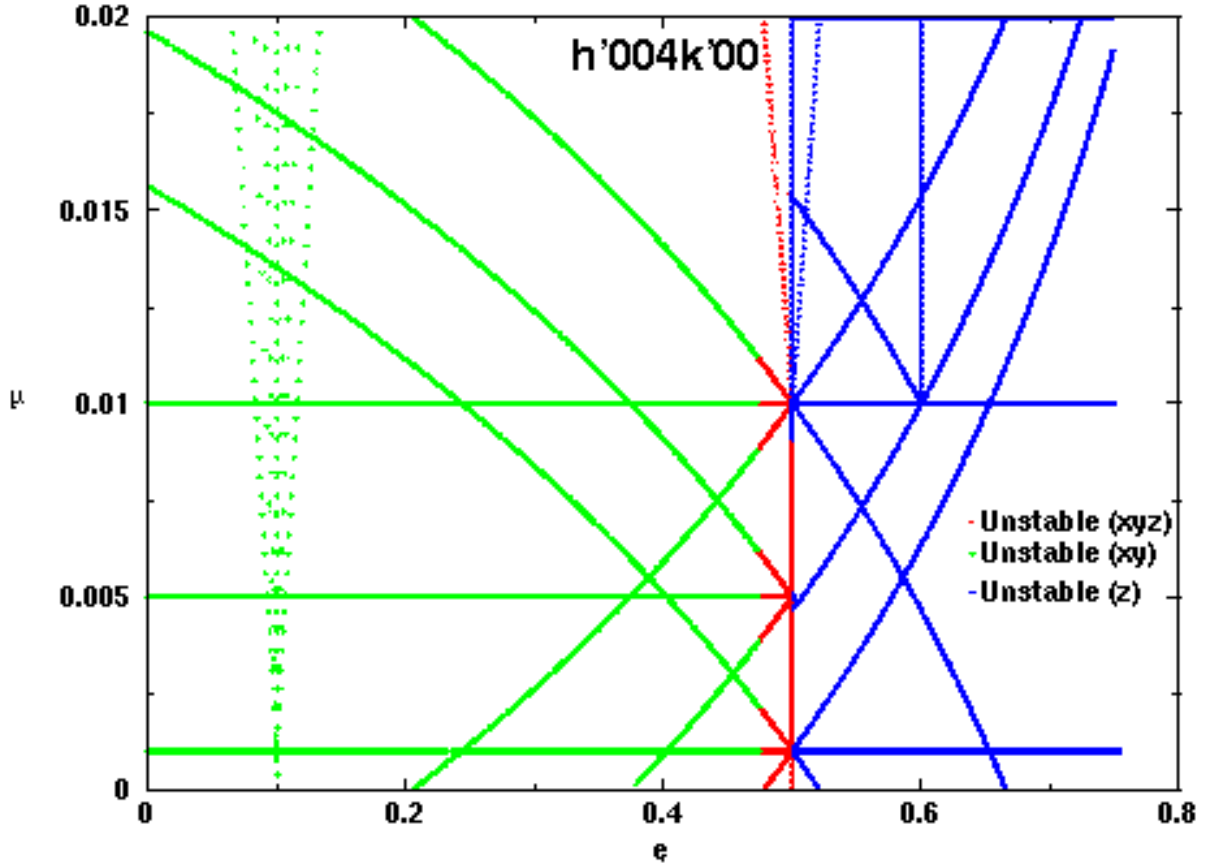


Fig. 4.— Continuation branches criss-crossing the phase-parameter space of the system. The starting RPO for all these branches is $h'004k'00$. This figure shows that in this case, for the chosen values of the mass-ratio and orbital eccentricity of the inner planet, there is no region of the parameter space which corresponds to stable resonant periodic orbits.

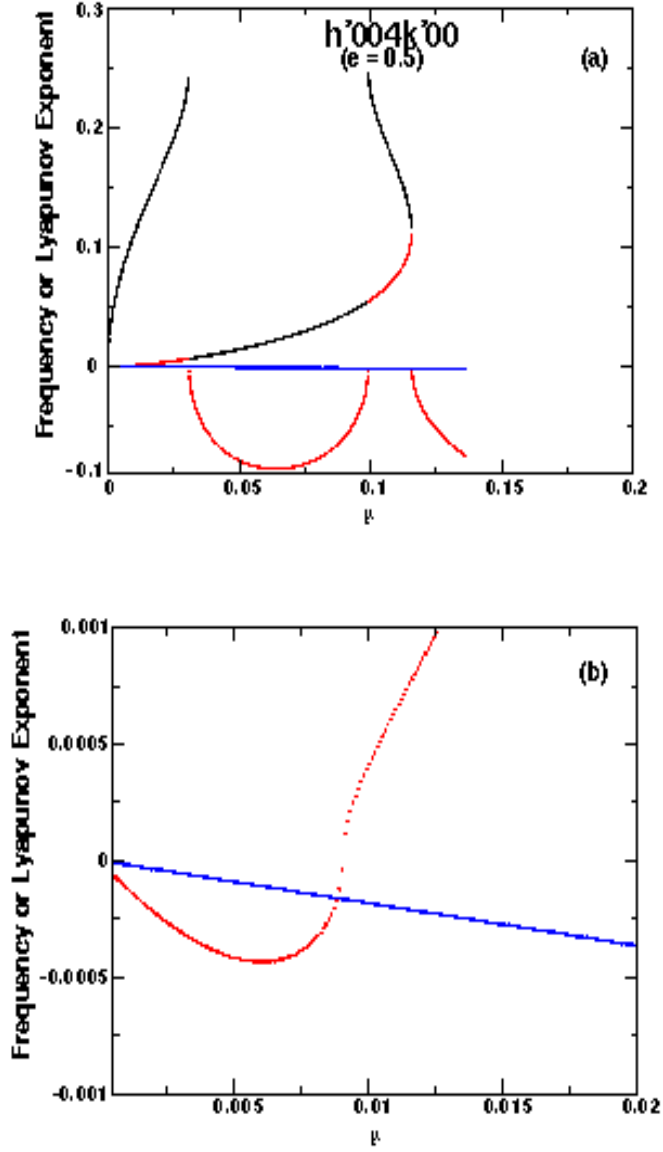


Fig. 5.— Frequency of libration (black) and secular libration (red) on the xy plane and the Lyapunov exponent along the z -axis (blue) of the outer body while the eccentricity of the inner planet is constant at 0.5. Figure 5b shows that for the values of the mass-ratio indicated in Figure 4, the system is unstable to both horizontal and vertical perturbations. While the system sustains its instability along the vertical direction, it becomes stable horizontally for $0.0091 \leq \mu \leq 0.03$ and $0.099 \leq \mu \leq 0.115$.

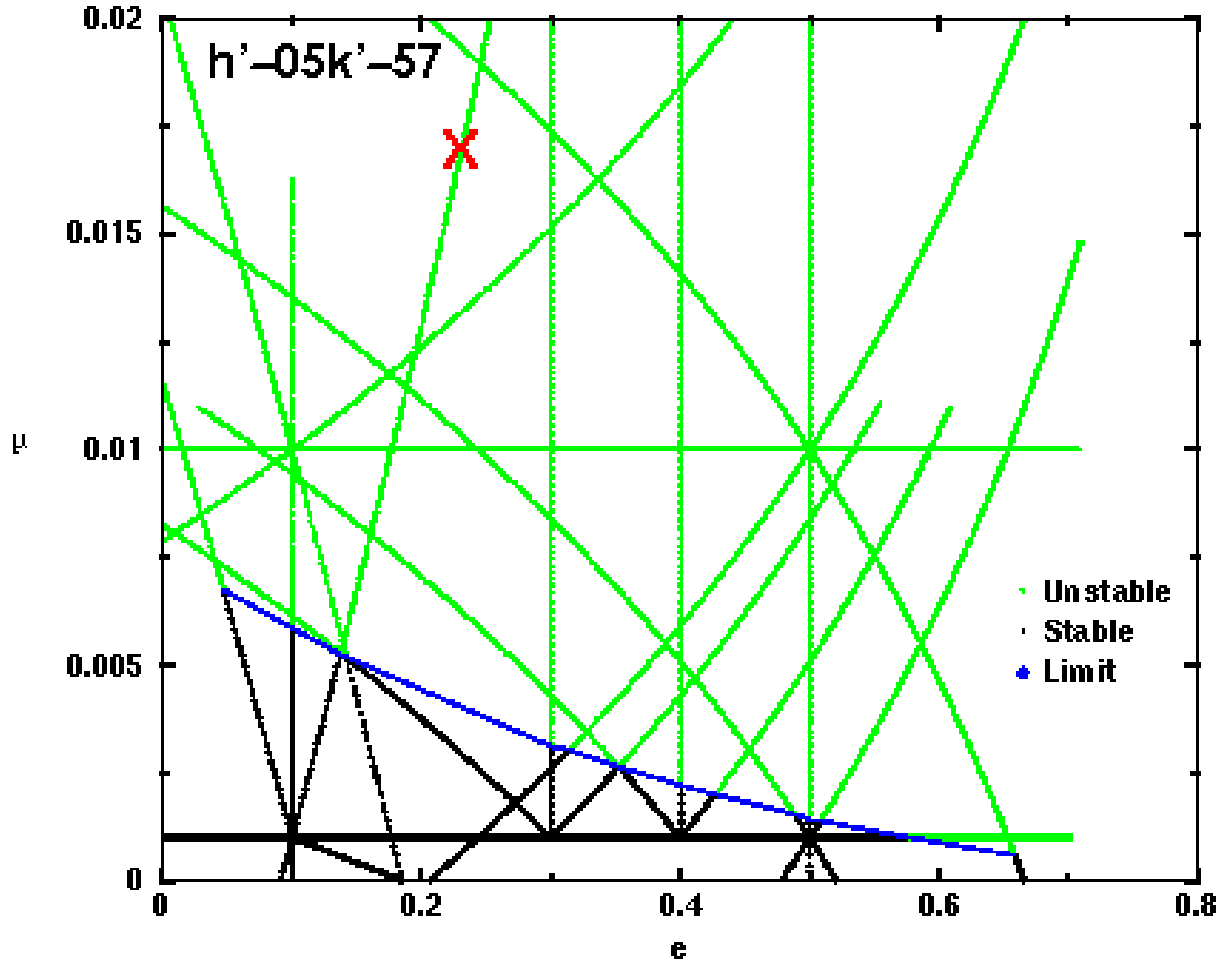


Fig. 6.— Criss-crossing the phase-parameter space of the system by continuation branches corresponding to the RPO, $h' - 05k' - 57$. One can see that in this case, there is a distinct region of the phase-parameter space where the resonant periodic orbits are stable.

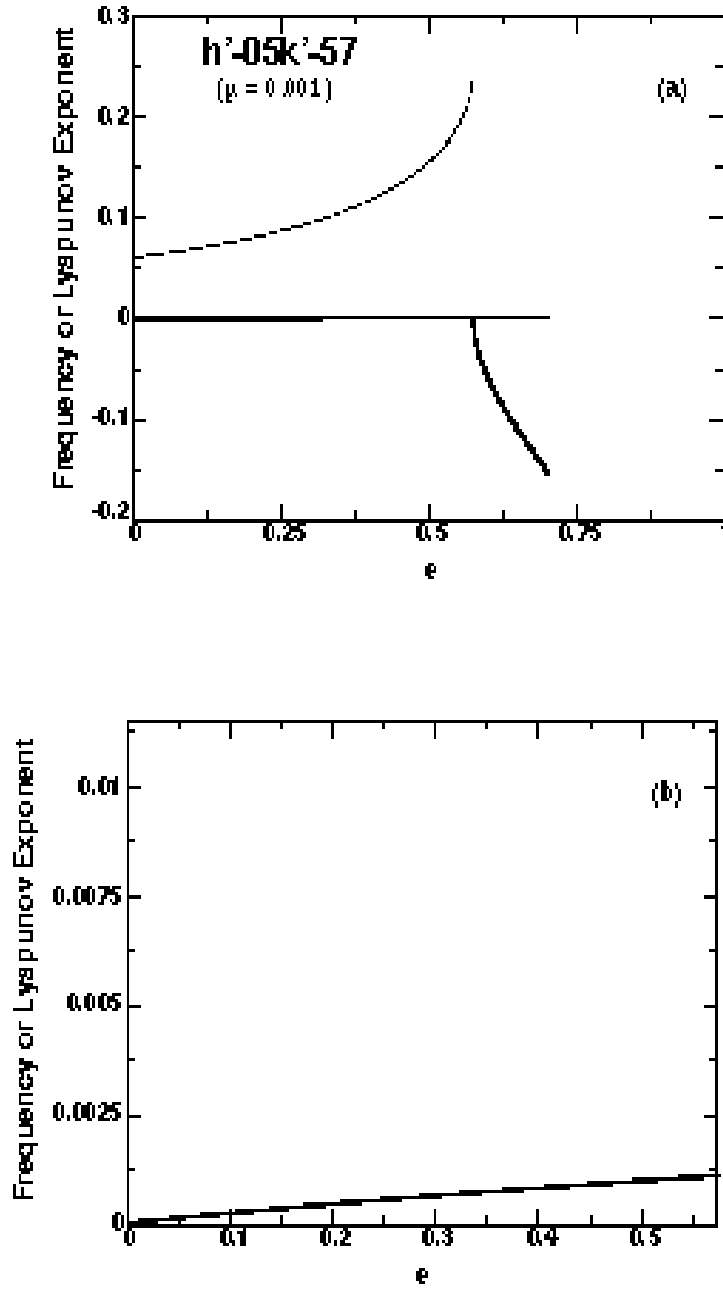


Fig. 7.— Frequency of libration (thin line) and secular libration (thick line) for the system of Figure 6 along the horizontal line of $\mu = 0.001$. As shown in Figure 7b, the orbit of the outer body is stable for the values of the orbital eccentricity of the outer planet smaller than 0.576.

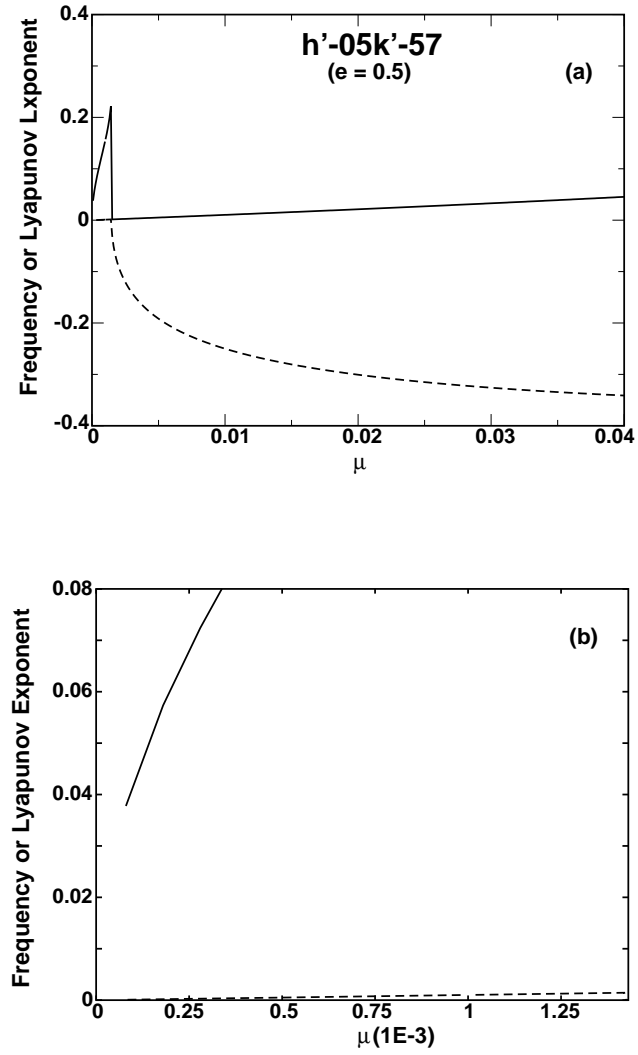


Fig. 8.— Frequencies of libration (solid line) and secular libration (dashed line) for the vertical line of $e = 0.5$ in Figure 6. As shown in Figure 8b, the orbit of the outer planet is stable for the values of the mass-ratio μ less than 0.0014.

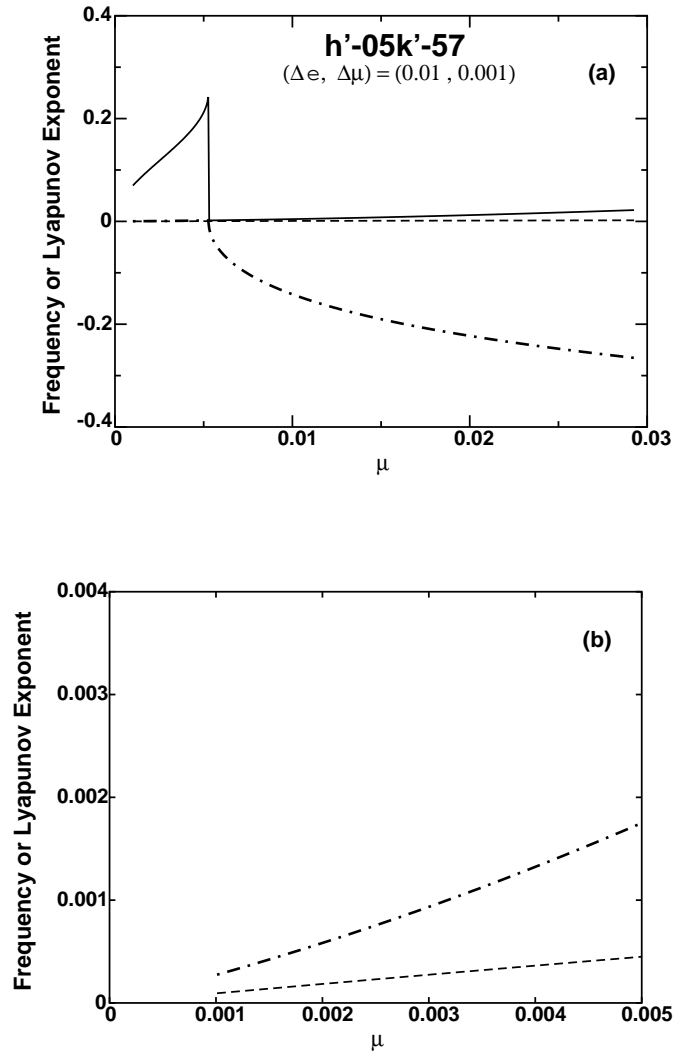


Fig. 9.— Frequencies of libration (solid line) and secular libration (dash-dotted line) and the Lyapunov exponent (dashed line) of the orbit of the outer body for the continuation path indicated by **X** in Figure 6. As shown in Figure 9b, the orbit of the outer planet is stable for the values of the mass-ratio less than 0.005.

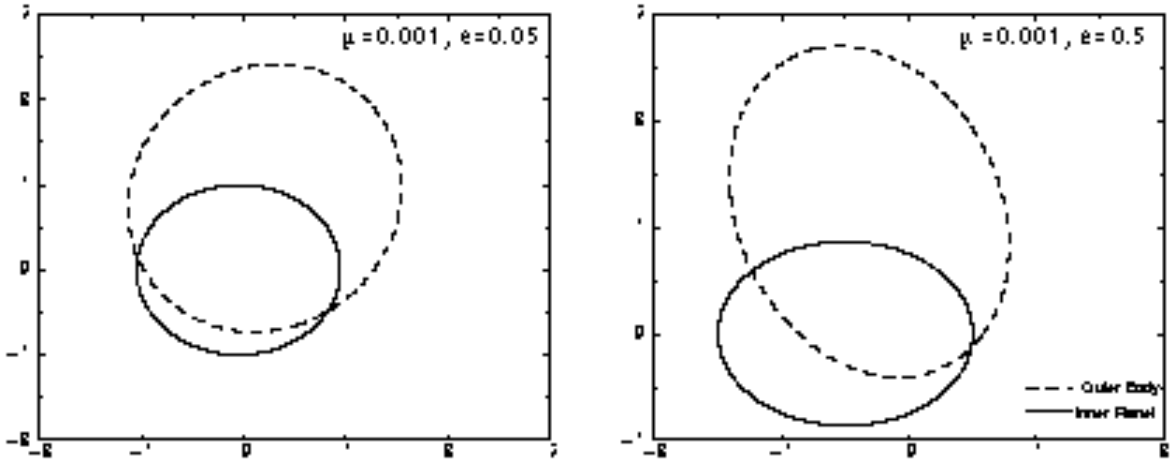


Fig. 10.— Resonant periodic orbits for $h'-05k'-57$.